Differences in Enantioselective Hydroxylation of 2,2′,3,6-Tetrachlorobiphenyl (CB45) and 2,2′,3,4′,6-Pentachlorobiphenyl (CB91) by Human and Rat CYP2B Subfamilies

Inui, Hideyuki ; Ito, Terushi ; Miwa, Chiharu ; Haga, Yuki ; Kubo, Makoto ; Itoh, Toshimasa ; Yamamoto, Keiko ; Miyaoka, Masayuki ; Mori,…

(Citation)
Environmental Science & Technology,56(14):10204-10215

(Issue Date)
2022-07-19

(Resource Type)
journal article

(Version)
Accepted Manuscript

Supporting Information

Differences in enantioselective hydroxylation of 2,2′,3,6-tetrachlorobiphenyl (CB45) and 2,2′,3,4′,6-pentachlorobiphenyl (CB91) by human and rat CYP2B subfamilies

Hideyuki Inui[1,2,], Terushi Ito[2], Chiharu Miwa[3], Yuki Haga[4], Makoto Kubo[5], Toshimasa Itoh[5], Keiko Yamamoto[5], Masayuki Miyaoka[6], Tadashi Mori[6], Harunobu Tsuzuki[2], Shintaro Mise[2], Erika Goto[2], Chisato Matsumura[4], Takeshi Nakano[7]*

[1]Biosignal Research Center, Kobe University, 1-1 Rokkodaicho, Nada-ku, Kobe, Hyogo 657-8501, Japan

[2]Graduate School of Agricultural Science, Kobe University, 1-1 Rokkodaicho, Nada-ku, Kobe, Hyogo 657-8501, Japan

[3]Faculty of Agriculture, Kobe University, 1-1 Rokkodaicho, Nada-ku, Kobe, Hyogo 657-8501, Japan

[4]Hyogo Prefectural Institute of Environmental Sciences, 3-1-18 Yukihiracho, Suma-ku, Kobe, Hyogo 654-0037, Japan

[5]Laboratory of Drug Design and Medicinal Chemistry, Showa Pharmaceutical University, 3-3165 Higashi-Tamagawagakuen, Machida, Tokyo 194-8543, Japan

[6]Graduate School of Engineering, Osaka University, 2-1 Yamadaoka, Suita, Osaka 565-0871, Japan

[7]Research Center for Environmental Preservation, Osaka University, 2-4 Yamadaoka, Suita, Osaka 565-0871, Japan

*Corresponding Author

Hideyuki Inui, Biosignal Research Center, Kobe University, 1-1 Rokkodaicho, Nada-ku, Kobe, Hyogo, 657-8501, Japan

E-mail: hinui@kobe-u.ac.jp, Telephone number: +81-78-803-5863

Number of Pages: 14

Number of Figures: 8

Number of Tables: 4

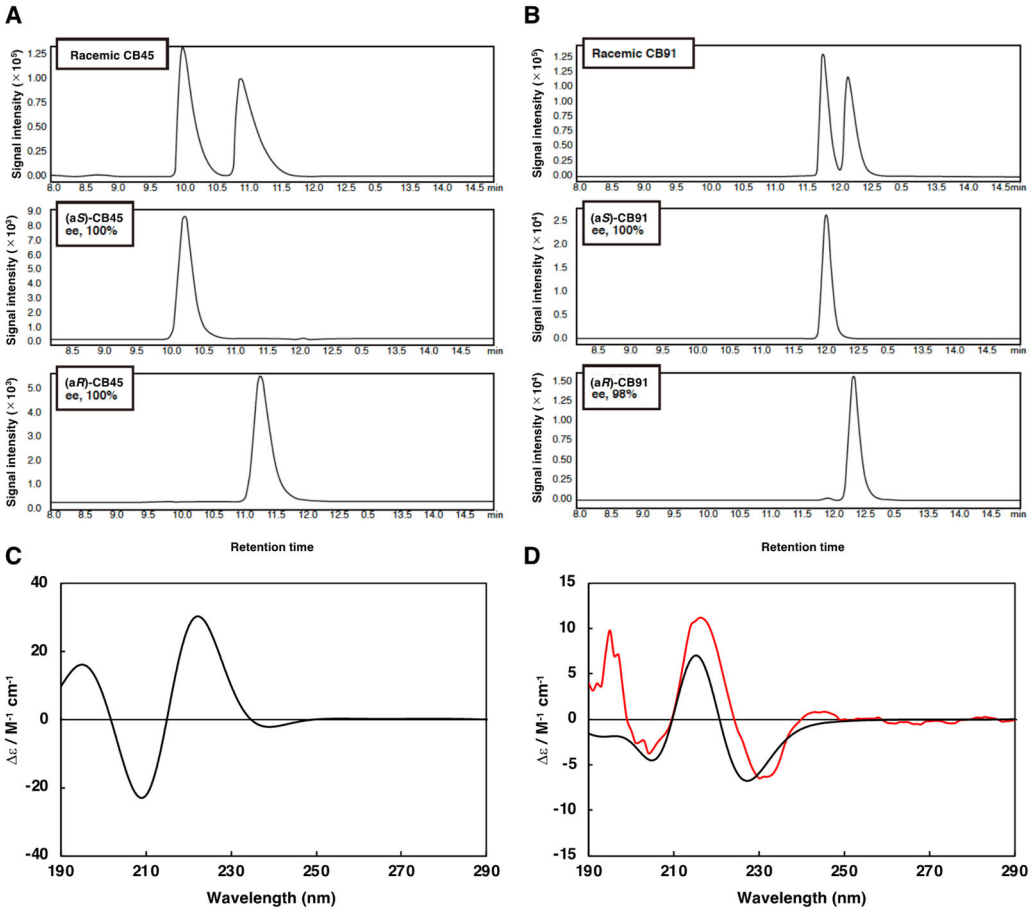

Figure S1 Isolation of atropisomers from racemic 2,2′,3,6-tetrachlorobiphenyl (CB45) (A) and 2,2′,3,4′,6-pentachlorobiphenyl (CB91) (B) and experimental (red) and theoretical (black) CD spectra of CB45 (C) and CB91 (D).

(a*S*)-CB45 and (a*S*)-CB91, and (a*R*)-CB45 and (a*R*)-CB91 were eluted in the first and second fractions, respectively. Enantiomeric excess (ee) values for each atropisomer were shown in the graphs. Experimental spectrum was obtained in hexane (ca. 7.7 μM) for the second fraction of CB91. Theoretical spectra for a*S* and a*R* atropisomers for CB45 and CB91 were calculated at the RI-CC2/aug-def2-TZVPP//B-LYP-D3/def2-TZVP level. The calculated rotational strengths in length gauge were scaled to one-half and were expanded by Gaussian functions and overlapped where the width of the band at 1/e height is fixed at 0.5 eV and the excitation energy was red-shifted by 0.6 eV.

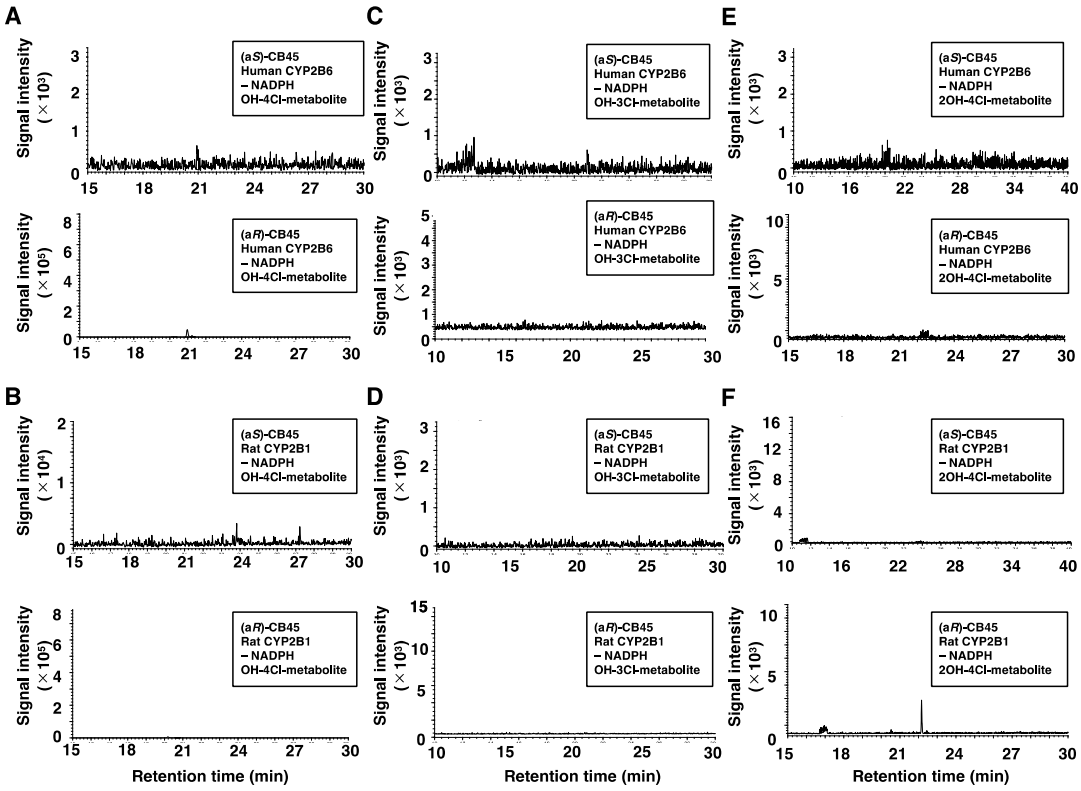

Figure S2 Chromatograms of mono-hydroxylated tetrachloro (A, B), mono-hydroxylated trichloro (C, D), and di-hydroxylated tetrachloro (E, F) metabolites produced from 2,2′,3,6-tetrachlorobiphenyl (CB45) by human CYP2B6 (A, C, E) and rat CYP2B1 (B, D, F), as analyzed by gas chromatography/ high-resolution mass spectrometry.

A, C, and E represent the metabolism of CB45 by human CYP2B6 without NADPH. B, D, and F show the metabolism of CB45 by rat CYP2B1 without NADPH. Upper and lower panels represent the metabolism of (a*S*)-CB45 and (a*R*)-CB45 as substrates, respectively.

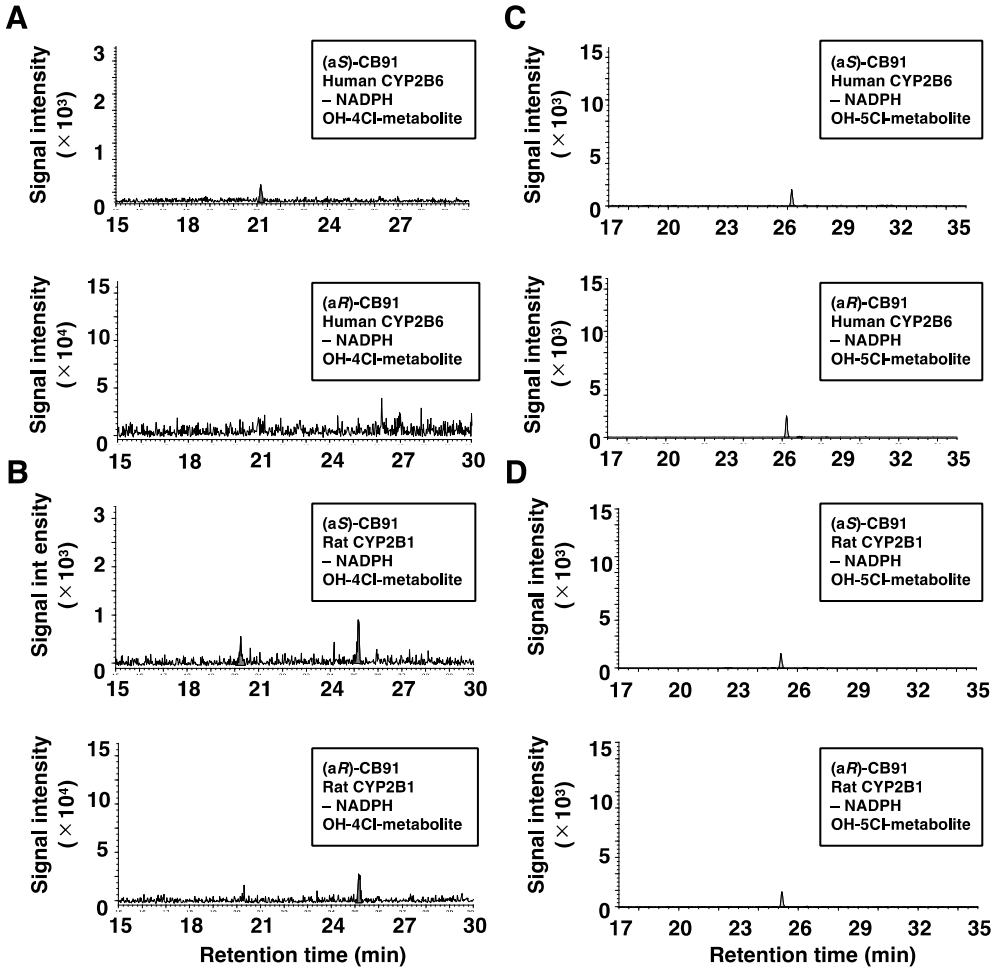

Figure S3 Chromatograms of mono-hydroxylated tetrachloro (A, B) and pentachloro (C, D) metabolites produced from 2,2′,3,4′,6-pentachlorobiphenyl (CB91) by human CYP2B6 (A, C) and rat CYP2B1 (B, D), as analyzed by gas chromatography/high-resolution mass spectrometry.

A and C represent the metabolism of CB91 by human CYP2B6 without NADPH. B and D represent the metabolism of CB91 by rat CYP2B1 without NADPH. Upper and lower panels represent the metabolism of (a*S*)-CB91 and (a*R*)-CB91 as substrates, respectively.

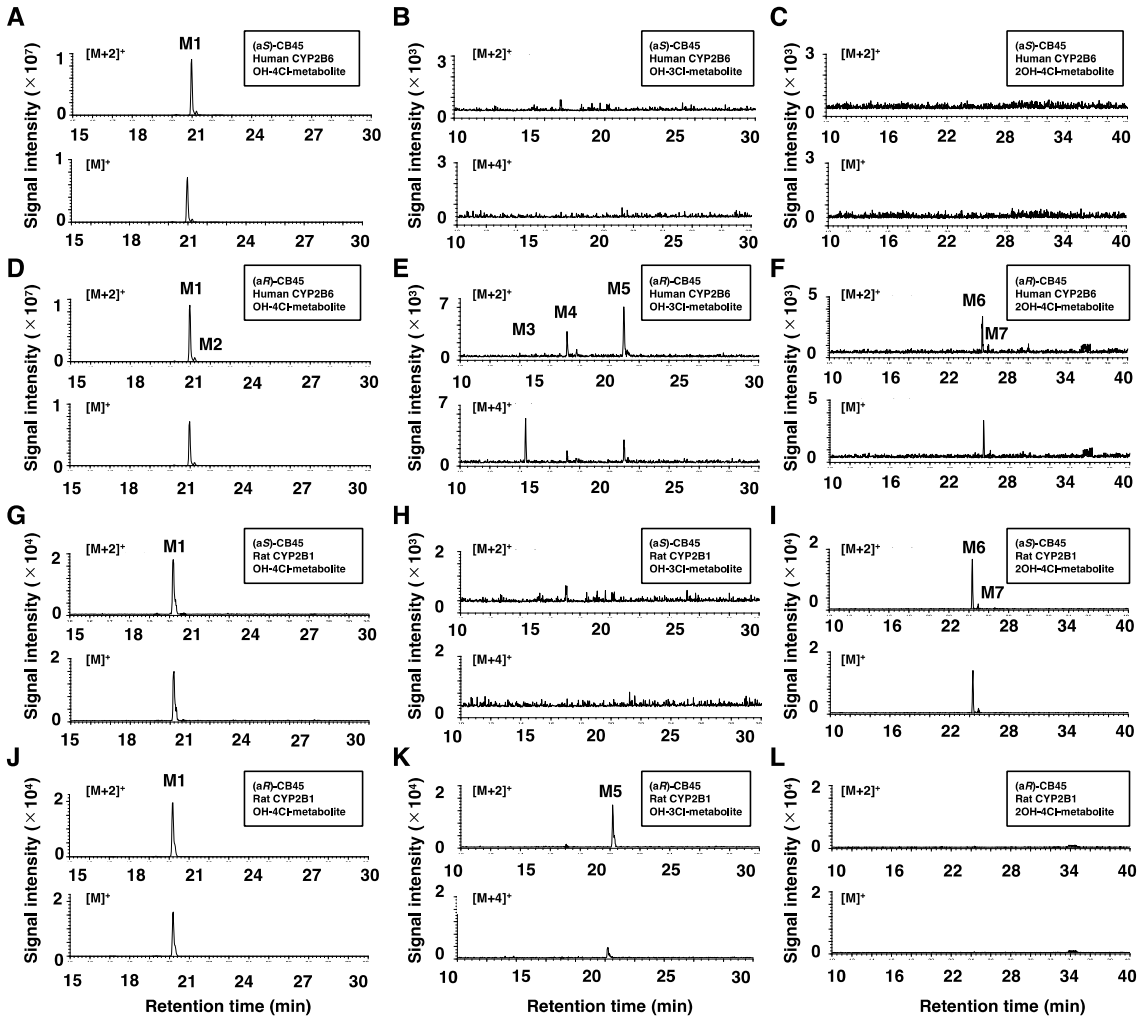

Figure S4 Isotope ratios of methylated 2,2′,3,6-tetrachlorobiphenyl (CB45) metabolites produced by human CYP2B6 (A–F) and rat CYP2B1 (G–L).

(a*S*)-CB45 (A–C, G–I) and (a*R*)-CB45 (D–F, J–L) were used as substrates. Hydroxylated tetrachloro (A, D, G, J), hydroxylated trichloro (B, E, H, K), and di-hydroxylated tetrachloro (C, F, I, L) metabolites were analyzed by gas chromatography/high-resolution mass spectrometry.

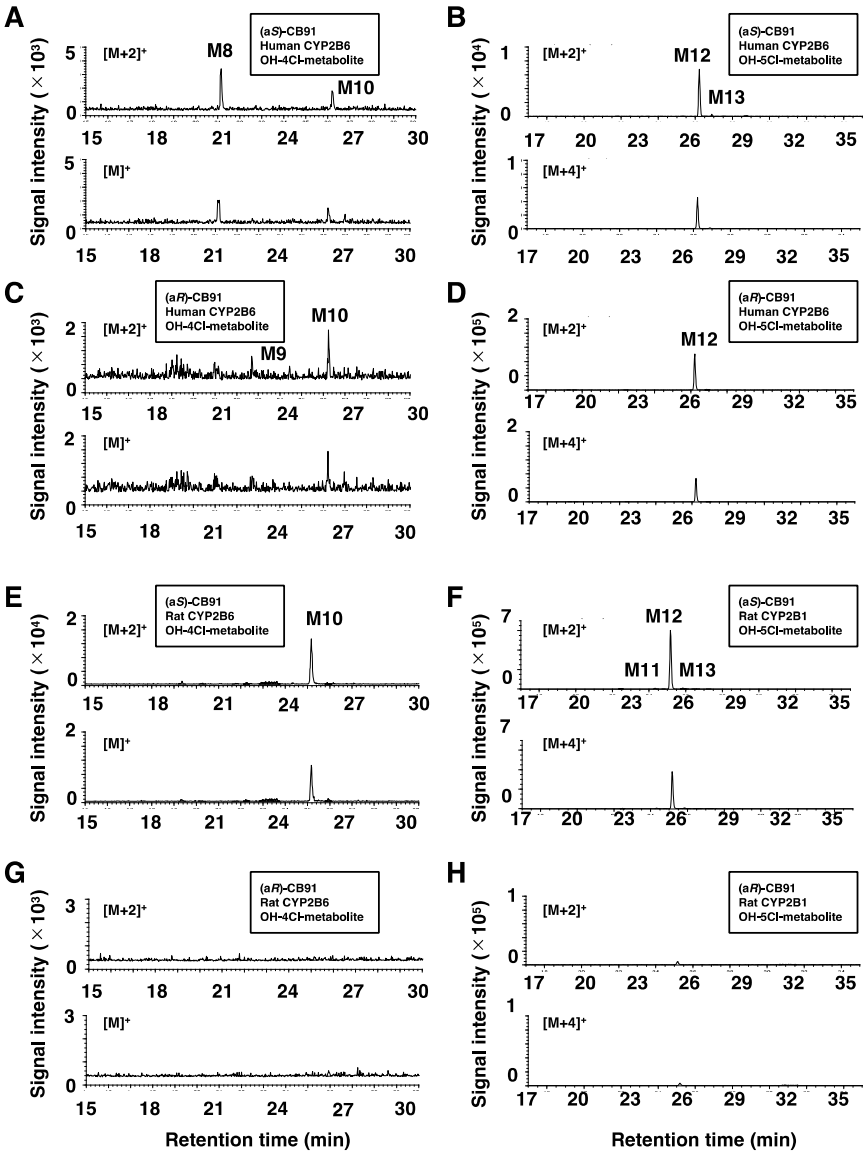

Figure S5 Isotope ratios of methylated 2,2′,3,4′,6-pentachlorobiphenyl (CB91) metabolites produced by human CYP2B6 (A–D) and rat CYP2B1 (E–H).

(a*S*)-CB91 (A, B, E, F) and (a*R*)-CB91 (C, D, G, H) were used as substrates. Hydroxylated tetrachloro (A, C, E, G), and hydroxylated pentachloro (B, D, F, H) metabolites were analyzed by gas chromatography/high-resolution mass spectrometry.

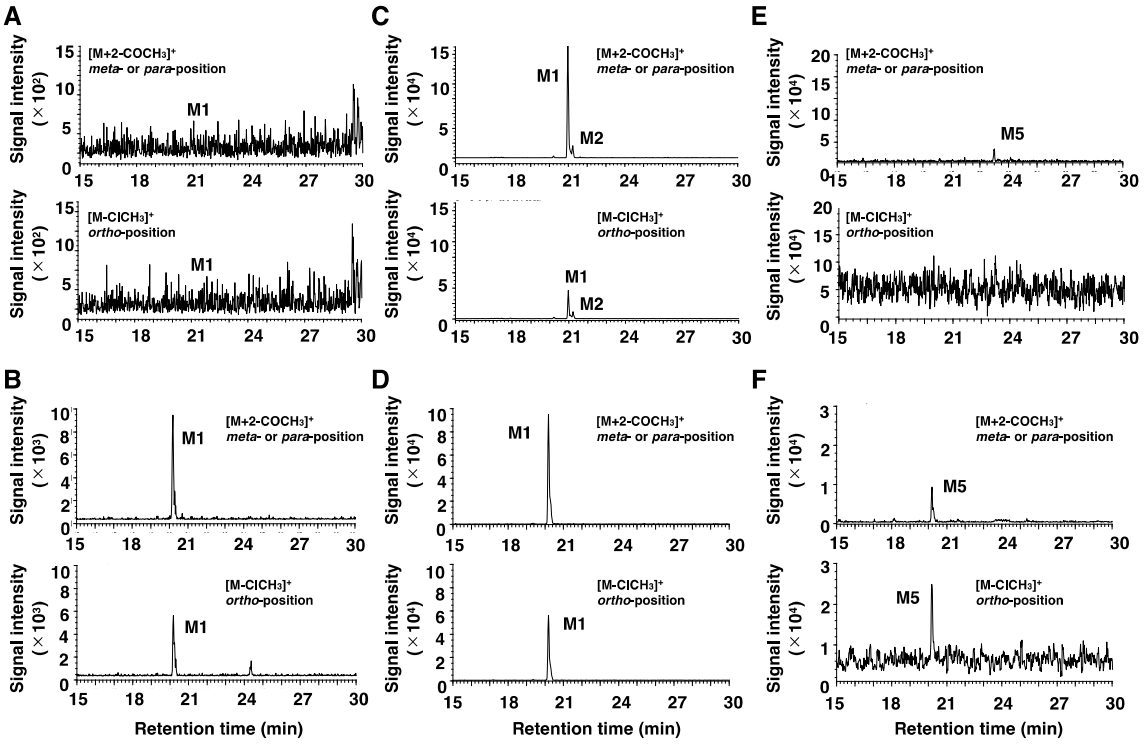

Figure S6 Patterns of fragment ions ($[M+2\text{-}COCH_3]^+$ and $[M\text{-}CH_3Cl]^+$) of mono-hydroxylated tetrachloro metabolites of (a*S*)-2,2′,3,6-tetrachlorobiphenyl (CB45) (A, B) and (a*R*)-CB45 (C, D) and mono-hydroxylated trichloro metabolites of (a*R*)-CB45 (E, F) produced on using human CYP2B6 (A, C, E) and rat CYP2B1 (B, D, F), as analyzed by gas chromatography/high-resolution mass spectrometry.

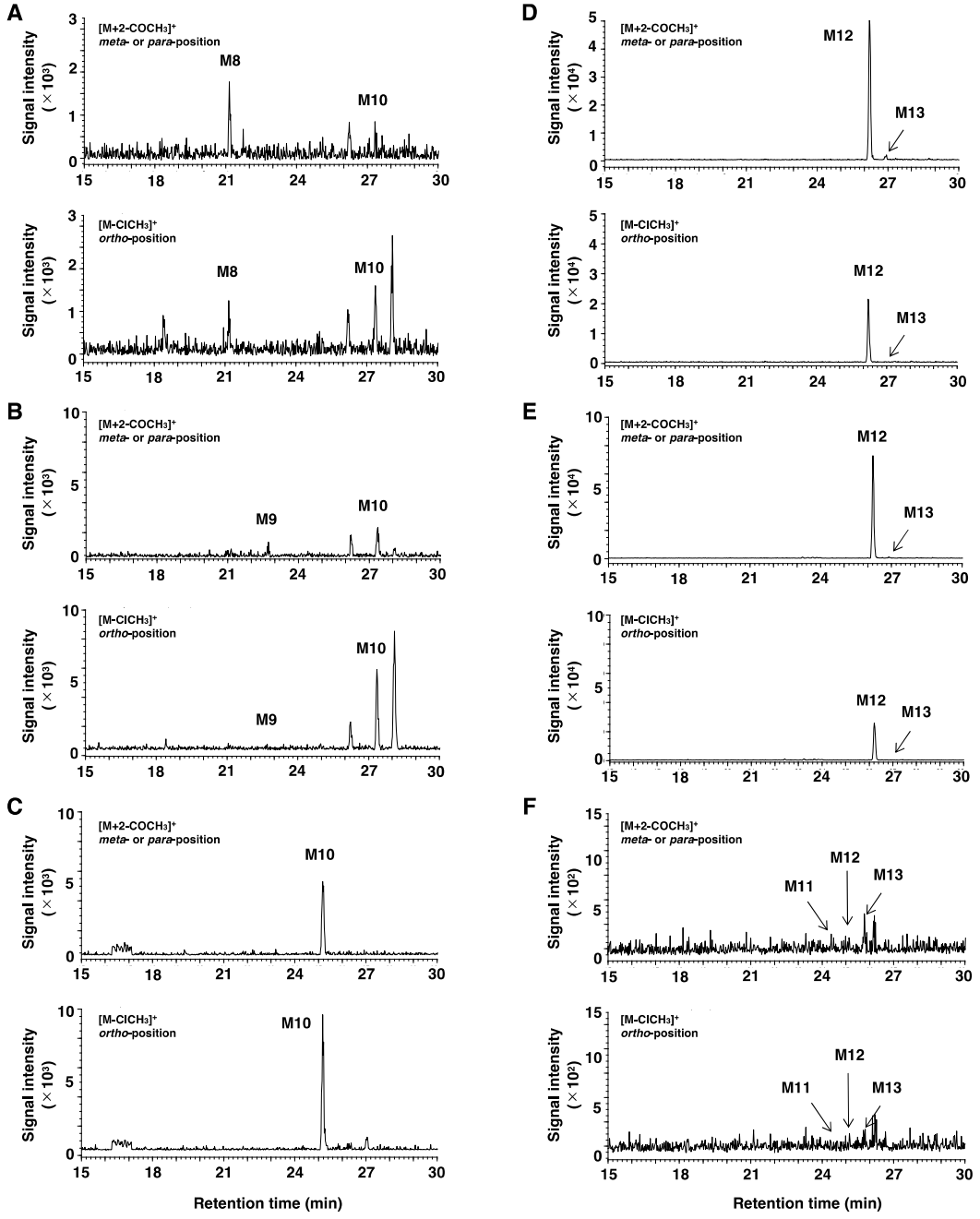

Figure S7 Patterns of fragment ions ($[M+2\text{-}COCH_3]^+$ and $[M\text{-}CH_3Cl]^+$) of mono-hydroxylated tetrachloro and pentachloro metabolites of (a*S*)-2,2′,3,4′,6-pentachlorobiphenyl (CB91) (A, C, D, F) and (a*R*)-CB91 (B, E) produced on using human CYP2B6 (A, B, D, E) and rat CYP2B1 (C, F), as analyzed by gas chromatography/high-resolution mass spectrometry.

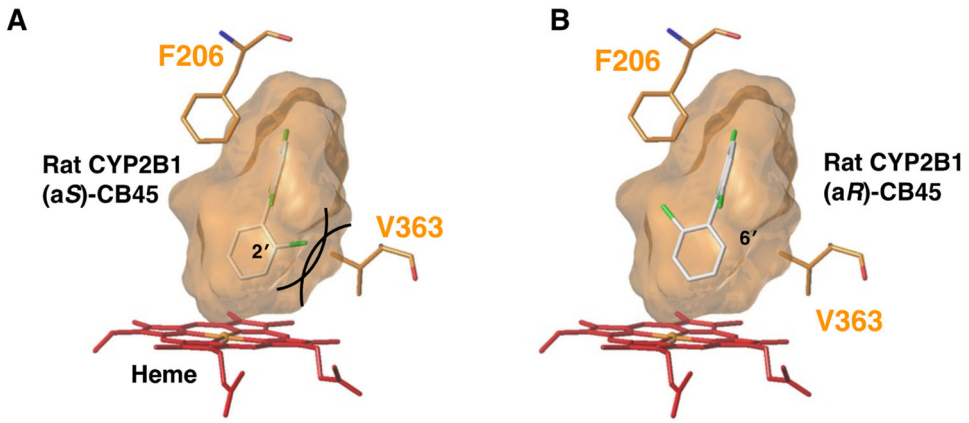

Figure S8 Rat CYP2B1 preferentially metabolizes (a*R*)-2,2′,3,6-tetrachlorobiphenyl (CB45).

Docking models of rat CYP2B1 toward (a*S*)-CB45 (A) and (a*R*)-CB45 (B) are described. The green stick in CB45 indicates a chlorine atom. Amino acids described in orange constitute the rat CYP2B1 substrate-binding cavity. Steric hindrance between chlorine at the 2′-position of (a*S*)-CB45 and a side chain of amino acids, such as V363, is observed in the rat CYP2B1 cavity.

Table S1. The analysis conditions for derivatized hydroxylated PCBs by gas chromatography/high-resolution mass spectrometry

	Condition
Gas chromatography	6890N (Agilent Technologies)
Mass spectrometry	JMS-800D (JEOL)
Column	HT8-PCB 60 m × 0.25 mm
Column temperature	130℃ (1 min) → (20℃ /min) → 210℃ → (2℃ /min) →285℃ → (30 ℃ /min) → 330 ℃
Inlet mode	Splitless (Purge starting time; 1.5 min)
Inlet temperature	290℃
Injection volume	2 μL
Carrier gas	1.2 mL/min
Interface temperature	290℃
Ion source temperature	280℃
Ionization voltage	38 eV
Detection mode	SIM

Table S2. Monitored ions of derivatized hydroxylated PCBs by high-resolution gas chromatography/high-resolution mass spectrometry

Homologue	Derivatized homologue	Selected fragment (*m/z*)
OH-TeCB[*1]	CH_3O-TeCBs	321.9301 $[M+2]^+$ 319.9329 $[M]^+$ 278.9116 $[M+2-COCH_3]^+$ 269.9406 $[M-ClCH_3]^+$
Di-OH-TeCB	Di-CH_3O-TeCBs	351.9406 $[M+2]^+$ 340.9435 $[M]^+$
OH-PeCB[*2]	CH_3O-PeCBs	355.8911 $[M+2]^+$ 357.8882 $[M+4]^+$ 312.8727 $[M+2-COCH_3]^+$ 305.8942 $[M+2-ClCH_3]^+$
OH-[$^{13}C_{12}$]-TeCB	CH_3O-[$^{13}C_{12}$]-TeCB	333.9702 $[M+2]^+$ 331.9732 $[M]^+$
OH-[$^{13}C_{12}$]-PeCB	CH_3O-[$^{13}C_{12}$]-PeCB	367.9313 $[M+2]^+$ 365.9342 $[M]^+$
[$^{13}C_{12}$]-2,3′,4′,5-TeCB[*3]		303.9597 $[M+2]^+$ 301.9626 $[M]^+$

[*1]Tetrachlorobiphenyl; [*2]Pentachlorobiphenyl; [*3]Syringe spike

Table S3. Retention times and retention time indexes for hydroxylated (OH)-metabolites of 2,2′,3,6-tetrachlorobiphenyl (CB45) and 2,2′,3,4′,6-pentachlorobiphenyl (CB91).

PCB	Metabolite	Retention time (Retention time index[*1])				Standard used for calibration curve
		Human CYP2B6		Rat CYP2B1		
		(a*S*)	(a*R*)	(a*S*)	(a*R*)	
CB45	M1	20.96 (0.7769)	20.98 (0.7779)	20.21 (0.7787)	20.21 (0.7786)	2-OH-2′,3,3′,4′-TeCB[*3]
	M2	-[*2]	21.23 (0.7870)	-	-	
	M3	-	14.41 (0.5340)	-	-	-[*4]
	M4	-	17.18 (0.6371)	-	-	
	M5	-	20.99 (0.7782)	-	20.21 (0.7789)	4-OH-2,3′,4-TrCB[*5]
	M6	-	25.40 (0.9415)	24.34 (0.9380)	-	2-OH-2′,3,3′,4′-TeCB
	M7	-	26.07 (0.9664)	24.91 (0.9599)	-	
CB91	M8	21.15 (0.7838)	-	-	-	2-OH-2′,3,3′,4′-TeCB
	M9	-	22.71 (0.8420)	-	-	
	M10	26.24 (0.9725)	26.24 (0.9727)	25.19 (0.9706)	-	4-OH-2,2′,3′,5-TeCB
	M11	-	-	24.34 (0.8929)	-	2-OH-3,3′,5,5′,6-PeCB[*6]
	M12	26.22 (0.9215)	26.22 (0.9271)	25.18 (0.9234)	-	
	M13	26.90 (1.026)	26.90 (1.026)	25.85 (1.027)	-	

[*1]Retention time indexes were represented by the relative retention time to [$^{13}C_{12}$]-4-OH-2′,3′,4′,5′-tetrachlorobiphenyl for M1–M10 and [$^{13}C_{12}$]-4-OH-2′,3,4′,5,5′-pentachlorobiphenyl for M11–M13.

[*2]Not detected.

[*3]Tetrachlorobiphenyl.

[*4]M3 and M4 were not quantified.

[*5]Trichlorobiphenyl.

[*6]Pentachlorobiphenyl.

Table S4. Isotope ratios of hydroxylated (OH)-metabolites of 2,2′,3,6-tetrachlorobiphenyl (CB45) and 2,2′,3,4′,6-pentachlorobiphenyl (CB91).

PCB	Metabolite (Cl number)	Isotope ratio				Theoretical ratio	Actual ratio (Standard)
		Human CYP2B6		Rat CYP2B1			
		(a*S*)	(a*R*)	(a*S*)	(a*R*)		
CB45	M1 (Tetra)	1:1.24 (M:M+2)	1:1.28 (M:M+2)	1:1.30 (M:M+2)	1:1.26 (M:M+2)	1:1.29 (M:M+2)	1:1.28 (4-OH-2,2′,3′,5-TeCB[*2])
	M2 (Tetra)	-[*1]	1:1.28 (M:M+2)	-	-	1:1.29 (M:M+2)	
	M3 (Tri)	-	0.04:1 (M+2:M+4)	-	-	3.06:1 (M+2:M+4)	3.00:1 (4-OH-2,3′,4′-TrCB[*3])
	M4 (Tri)	-	2.26:1 (M+2:M+4)	-	-	3.06:1 (M+2:M+4)	
	M5 (Tri)	-	2.94:1 (M+2:M+4)	-	3.44:1 (M+2:M+4)	3.06:1 (M+2:M+4)	
	M6 (Tetra)	-	1:1.24 (M:M+2)	1:1.33 (M:M+2)	-	1:1.29 (M:M+2)	1:1.28 (4-OH-2,2′,3′,5-TeCB)
	M7 (Tetra)	-	1:1.19 (M:M+2)	1:1.06 (M:M+2)	-	1:1.29 (M:M+2)	
CB91	M8 (Tetra)	1:1.33 (M:M+2)	-	-	-	1:1.29 (M:M+2)	1:1.28 (4-OH-2,2′,3′,5-TeCB)
	M9 (Tetra)	-	1:1.27 (M:M+2)	-	-	1:1.29 (M:M+2)	
	M10 (Tetra)	1:1.12 (M:M+2)	1:1.28 (M:M+2)	1:1.24 (M:M+2)	-	1:1.29 (M:M+2)	
	M11 (Penta)	-	-	1.61:1 (M+2:M+4)	-	1.55:1 (M+2:M+4)	1.63:1 (3-OH-2,3′,4,4′,6-PeCB[*4])
	M12 (Penta)	1.56:1 (M+2:M+4)	1.57:1 (M+2:M+4)	1.58:1 (M+2:M+4)	-	1.55:1 (M+2:M+4)	
	M13 (Penta)	1.44:1 (M+2:M+4)	1.60:1 (M+2:M+4)	1.79:1 (M+2:M+4)	-	1.55:1 (M+2:M+4)	

[*1]Not detected.

[*2]Tetrachlorobiphenyl.

[*3]Trichlorobiphenyl.

[*4]Pentachlorobiphenyl.